JOURNAL OF BACTERIOLOGY, Oct. 2004, p. 6605–6616 Vol. 186, No. 19
0021-9193/04/$08.00+0 DOI: 10.1128/JB.186.19.6605–6616.2004
Copyright © 2004, American Society for Microbiology. All Rights Reserved.

Transcription Regulation by the *Mycobacterium tuberculosis* Alternative Sigma Factor SigD and Its Role in Virulence†

Sahadevan Raman,[1] Rohan Hazra,[1]‡ Christopher C. Dascher,[2] and Robert N. Husson[1]*

Division of Infectious Diseases, Children's Hospital of Boston,[1] and Rheumatology and Immunology Division, Brigham & Women's Hospital,[2] Harvard Medical School, Boston, Massachusetts

Received 12 April 2004/Accepted 2 July 2004

***Mycobacterium tuberculosis*, an obligate mammalian pathogen, adapts to its host during the course of infection via the regulation of gene expression. Of the regulators of transcription that play a role in this response, several alternative sigma factors of *M. tuberculosis* have been shown to control gene expression in response to stresses, and some of these are required for virulence or persistence in vivo. For this study, we examined the role of the alternative sigma factor SigD in *M. tuberculosis* gene expression and virulence. Using microarray analysis, we identified several genes whose expression was altered in a strain with a *sigD* deletion. A small number of these genes, including *sigD* itself, the gene encoding the autocrine growth factor RpfC, and a gene of unknown function, Rv1815, appear to be directly regulated by this sigma factor. By identifying the in vivo promoters of these genes, we have determined a consensus promoter sequence that is putatively recognized by SigD. The expression of several genes encoding PE-PGRS proteins, part of a large family of related genes of unknown function, was significantly increased in the *sigD* mutant. We found that the expression of *sigD* is stable throughout log phase and stationary phase but that it declines rapidly with oxygen depletion. In a mouse infection model, the *sigD* mutant strain was attenuated, with differences in survival and the inflammatory response in the lung between mice infected with the mutant and those infected with the wild type.**

Mycobacterium tuberculosis is an obligate mammalian pathogen that is believed to infect roughly one-third of the world's population (33). While capable of causing disease in a substantial proportion of those infected, resulting in approximately eight million cases of active tuberculosis in the world each year, this bacillus causes an asymptomatic infection in most individuals. After an initial period of rapid replication, the infection is typically contained by the host immune system, resulting in the apparent eradication of the infection in some individuals but in the persistence of small numbers of bacteria in others, resulting in asymptomatic chronic infections. These latent infections may subsequently become active, often in the setting of decreased host immunity, with increased bacterial replication and extensive tissue damage.

During these several stages of infection, *M. tuberculosis* encounters a changing host environment, in response to which the bacillus must activate defense and repair mechanisms and reprogram its physiology to ensure survival. The large number of putative transcription regulators identified in the *M. tuberculosis* genome sequence indicate that much of the regulation required for these adaptations by *M. tuberculosis* occurs at the level of transcription (6). Among the transcription regulators that have been implicated in these processes are the alternative sigma factors of this organism, 12 of which are encoded in the *M. tuberculosis* genome. In previous work, our laboratory and others have implicated several alternative sigma factors in the mycobacterial response to a variety of stresses, most notably oxidative stress (13, 17–19, 24, 34). A role for alternative sigma factor-regulated gene expression in stationary-phase adaptation and in vivo replication in late-stage infections in mice has also been demonstrated (5, 11).

In addition to oxidative and nitrosative stresses, in vitro models of *M. tuberculosis* infection and latency have focused on two environmental conditions that are thought to be encountered by *M. tuberculosis* during infection, i.e, nutrient limitation (starvation) and hypoxia. A shift in carbon source utilization requiring the enzyme isocitrate lyase has been associated with the ability of *M. tuberculosis* to persist in vivo (20). Similarly, an intact *relA* gene, encoding ppGpp synthase, which is required for the induction of the stringent response, has been shown to be essential for the in vivo persistence of *M. tuberculosis* in mice (8). The expression of *sigD* appears to be linked to the stringent response, with an increased expression in response to starvation that is at least partly Rel dependent (3, 8). Microarray data have demonstrated substantial, though incomplete, similarities between the *M. tuberculosis* transcription profiles produced in response to hypoxia, sublethal concentrations of nitric oxide, and macrophage infection (26, 27, 31). In contrast, these transcription responses show little overlap with starvation- or stringent response-induced alterations in transcription. These data suggest that both hypoxia and starvation are important for *M. tuberculosis* survival in vivo but that they provoke distinct physiologic adaptations that may be relevant at different stages of the dynamic process of infection by *M. tuberculosis*.

In this work, we present an initial characterization of the *M. tuberculosis* alternative sigma factor SigD. After constructing a *sigD* deletion (Δ*sigD*) strain of *M. tuberculosis*, we examined

* Corresponding author. Mailing address: Children's Hospital, Division of Infectious Diseases, 300 Longwood Ave., Boston, MA 02115. Phone: (617) 355-5151. Fax: (617) 730-0254. E-mail: robert.husson@childrens.harvard.edu.

† Supplemental material for this article may be found at http://jb.asm.org.

‡ Present address: HIV and AIDS Malignancy Branch, National Cancer Institute, Bethesda, MD 20892.

the role of this sigma factor in growth and viability in vitro and its effects on global and specific gene transcription. Using in vivo promoter analysis, we have identified a consensus SigD recognition sequence. Using a mouse model of infection, we assessed the role of this sigma factor in *M. tuberculosis* virulence. Based on the identity of genes that it regulates, its effects on global transcription, and the response of its gene to starvation and hypoxia, our data indicate that this sigma factor plays a role in optimal growth both under nutrient replete conditions and, paradoxically, in response to starvation. These data suggest that SigD, while nonessential for viability in vitro, may play a role at several stages during infection to optimize bacterial replication and survival.

MATERIALS AND METHODS

Bacterial strains and culture conditions. *M. tuberculosis* H37Rv was used as the parental strain for generating an isogenic Δ*sigD* strain and as the wild type (wt) for all experiments. *Escherichia coli* DH5α (Life Technologies) and XL1 Blue (Stratagene) were used as host strains for cloning experiments. *Mycobacterium smegmatis* strain mc^2-155 or its derivatives were used for all experiments involving this mycobacterial species (29). *M. tuberculosis* and *M. smegmatis* were grown in flasks with shaking or as standing cultures in Middlebrook 7H9 broth supplemented with albumin-dextrose complex (7H9-ADC) plus 0.05% Tween 80 and 0.2% glycerol. For hypoxia studies, the uniform gradual oxygen depletion model of Wayne and Hayes was used, as described below (32). Colony counts from mouse organs were performed by plating bacteria on Middlebrook 7H11 selective agar medium (Hardy Diagnostics). *E. coli* was grown on L agar or in L broth. Ampicillin (100 μg/ml), apramycin (30 μg/ml), kanamycin (50 μg/ml), and zeocin (50 μg/ml) were added to culture media as indicated.

Construction of *M. tuberculosis sigD* mutant strain and complementation of the mutation. The *M. tuberculosis sigD* mutant was constructed by targeted mutagenesis with the temperature-sensitive *sacB* counterselection system. Briefly, the *sigD* gene, from annotated codon 22 through codon 201, was removed by overlap PCR and replaced with a kanamycin resistance gene. The resulting disrupted gene and flanking DNA were sequenced and blunt cloned into the XbaI site of pRH1351, a derivative of pPR23 harboring the *sacB* and *xylE* genes (7, 22, 24). The resulting vector, pRH1450, was electroporated into *M. tuberculosis* H37Rv. The recombinants were selected at 30°C on kanamycin plates. Individual colonies were picked, grown at the permissive temperature in broth culture, and then plated on plates containing 10% sucrose at 39°C. The resulting colonies were screened for XylE activity as described previously (7). Genomic DNAs from *xylE*-negative colonies were analyzed by PCR, and the presence of the *sigD* deletion and the absence of the wt allele were confirmed by Southern analysis.

To complement the *sigD* mutation, we placed an intact copy of *sigD* in an apramycin-resistant derivative of the integrating vector pMH94 (15, 24). Because of previous results indicating poor expression from this type of construct (24), the constitutive *hsp70* promoter was placed 5′ of the *sigD* coding sequence. This construct was electroporated into the *sigD* mutant, followed by plating and selection for apramycin-resistant colonies. The presence of the intact *sigD* allele was confirmed by PCR.

RNA isolation and primer extension. Total RNAs were isolated from wt *M. tuberculosis* and the Δ*sigD* mutant strains grown to mid-log phase (optical density at 600 nm [OD_{600}], 0.4). The bacterial cells from 50 ml of culture were centrifuged, and the pellet was resuspended in 1 ml of Trizol (Invitrogen) and transferred to a 2 ml-tube containing ceramic and silica beads. The tubes were agitated in an FP120 instrument (QBiogene) or in a bead beater (Biospec), with cooling of the tubes on ice between each agitation. The lysate was removed and place into a fresh tube, and RNA was prepared according to the supplier's recommendations (Invitrogen). The final RNA pellet was dissolved in water and treated with DNase I. The DNase-treated RNA was further purified by use of an RNeasy clean-up kit according to the manufacturer's protocol (Qiagen).

For primer extension analysis, 0.5 pmol of a γ-^{32}P-labeled primer (*sigD* [5′-CACGGCCTCCGCAACCACAGCGTCGAGA-3′], *rpfC* [5′-CGTGGGCAACGGCGGTGGAGAGCGACAT-3′], or Rv1815 [5′-GGATTTCCATGCCGGGGAACACCAAGAC-3′]) was mixed with 5 μg of RNA in a 6-μl volume, and reverse transcription (RT) was performed as previously described (24). The reaction products were separated by polyacrylamide gel electrophoresis in a sequencing gel. Sequencing reactions, performed with the same primer used for primer extension, were run in adjacent lanes to determine the sizes of the transcripts generated. Transcripts were quantified with a phosphorimager and ImageQuant software (Molecular Dynamics).

Microarray experiments and analysis. *M. tuberculosis* PCR arrays and oligoarrays were used to identify SigD-regulated genes. PCR arrays, provided by Eric Rubin, were produced with gene-specific PCR products generated by the use of amino-modified primers coupled to aldehyde-coated 3D-Link slides (Motorola) (25). The *M. tuberculosis* oligoarrays were obtained from The Institute for Genomic Research (TIGR) through the National Institute of Allergy and Infectious Diseases-sponsored Pathogen Functional Genomics Resource Center. These microarrays consisted of 4,750 70-mer oligonucleotides representing 4,127 open reading frames from *M. tuberculosis* strain H37Rv and 623 unique open reading frames from strain CDC1551 that are not present in the H37Rv strain's annotated gene complement. RNAs were prepared as described above, and cDNAs were synthesized by RT with Superscript II (Invitrogen) and amino-allyl dUTP incorporation, followed by coupling to Cy-3 or Cy-5 fluorescent dyes (Amersham). TIGR protocols were followed for probe synthesis, hybridization, and washing procedures (http://www.tigr.org/tdb/microarray/protocolsTIGR.shtml). The hybridized slides were scanned with an Axon 4000B scanner, and spot intensities were defined and quantified with Genepix software (Axon, Union City, Calif.).

Four hybridization values from oligoarray experiments (two replicates from each of two independent RNA preparations) were used for statistical analysis. The raw data median values were normalized as described by Churchill and colleagues (14). The data were reformatted to use the signals from duplicate spots. Statistical analysis was performed with the National Institute of Aging array analysis tool (http://lgsun.grc.nia.nih.gov/ANOVA/). We used the most conservative error model, the maximum of averaged and actual error variance, in order to reduce the number of false-positive results. Up-regulated and down-regulated genes were selected based on false discovery rates (FDRs) of <0.05 (FDR = $P \times N$/rank, where P is the P value, N is the total number of genes, and rank is the rank of the gene, as ordered by increasing P values).

Real-time PCR and mRNA quantitation. RNAs extracted from *M. tuberculosis* H37Rv grown under several conditions were prepared as described above, except that an additional DNase treatment was added. Primers were designed with Primer Express software (Applied Biosystems), and RT-PCR was performed by use of an iScript cDNA synthesis kit, iTaq SYBR green reagents (Bio-Rad), and an ABI7000 sequence detection instrument. Duplicate reactions containing 100 ng of template were performed for *sigD* and other genes of interest. The expression of *sigA* was quantified for each sample to allow for comparisons with the relatively stable expression of this gene (17). An RNA sample that had not been reverse transcribed was included in all experiments to exclude significant DNA contamination. Standard curves were obtained by performing PCRs with SYBR green detection on serial dilutions of spectrophotometrically quantified genomic DNA or plasmid DNA. *hspX* was used as a positive control for oxygen depletion experiments.

Oxygen depletion experiments. For RT-PCR experiments and viability studies, the stirred model of gradual oxygen depletion was used (32). Early-log-phase cultures of bacteria were inoculated into 25-ml sealed bottles with 17 ml of medium and a stir bar (headspace ratio = 0.5). The bottles were stirred by use of a magnetic stir plate at low speed to keep the cells in suspension and to keep the dissolved oxygen concentration uniform in the medium. One set of cultures was harvested at each time point for RNA extraction, and a second set of cultures was used for plating serial dilutions.

Computer database searching. Searches of the *M. tuberculosis* H37Rv genome sequence for consensus promoter elements were performed by utilizing the "search pattern" program available at the TubercuList web site of the Pasteur Institute (http://genolist.pasteur.fr/TubercuList) and the motif-finding function of the Bio prospector program (http://robotics.stanford.edu/~xsliu/BioProspector/).

Oxidative stress and isoniazid exposure. Susceptibilities to diamide, plumbagin, cumene hydroperoxide, and isoniazid (INH) were determined by a disk diffusion assay as previously described (24). Plating efficiency experiments were performed with Middlebrook 7H10 agar supplemented with ADC enrichment and 0.05 μg of INH/ml. To determine the effect of INH on gene expression, we grew broth cultures to mid-exponential phase (OD_{600} = 0.4 to 0.5), split the cultures into two aliquots, added INH to one aliquot at a concentration of 1 μg/ml, and incubated the cultures for 4 h prior to RNA isolation as described above.

Mouse infection and virulence assay. Six-week-old BALB/c mice were purchased from Jackson Laboratory (Bar Harbor, Maine). All mice were housed in microisolator cages in a biosafety level 3 animal facility at the Dana Farber Cancer Institute (Boston, Mass.) under specific-pathogen-free conditions. A vial of frozen bacteria was thawed to room temperature and then dispersed by

sonication in a cup horn sonicator twice for 10 s. The bacterial suspension was then triturated through a 27-gauge insulin syringe three times to disrupt clumps. The bacteria were then diluted to 10^7 CFU/ml in 0.9% saline with 0.02% Tween 80. Twelve mice from each group were injected with 10^6 CFU in the lateral tail vein. The weights and morbidity of the mice were monitored for the survival experiment. Mice that became moribund were euthanized, with the time of survival counted until the day of euthanasia.

For bacterial replication and histopathology experiments, six mice from each group were sacrificed after 9, 24, and 59 days. The right lungs were removed and homogenized in saline-Tween by use of a bead beater. Serial dilutions of the homogenates were plated for CFU, and colonies were counted after 3 to 4 weeks at 37°C. For histological studies, the left lungs were removed and fixed for at least 48 h in 10% buffered formalin. The tissues were processed and embedded in paraffin. Tissues for slides were cut into 5-μm-thick sections and then stained with hematoxylin and eosin or acid fast stained for bacteria by standard techniques. All mouse experiments were performed according to protocols approved by the Animal Care and Use Committees of Children's Hospital Boston and the Dana Farber Cancer Institute.

For all data presented, representative results of one experiment are shown, with all experiments repeated at least once to confirm the results.

RESULTS

Construction of Δ*sigD* mutant and complemented strains of *M. tuberculosis* and identification of SigD-regulated genes. A deletion of the *sigD* coding sequence from annotated codon 22 through codon 201 was created, and a kanamycin resistance gene was inserted. This deletion allele was introduced into the chromosome of H37Rv by homologous recombination, with counterselection to achieve replacement of the wt allele, as described in Materials and Methods. Gene replacement was confirmed by Southern blot analysis of the genomic DNA. To create a strain in which the Δ*sigD* mutation was complemented, we introduced a single copy of the intact *sigD* coding region into the chromosome at the phage L5 *attB* site (15), as described in Materials and Methods. Expression of *sigD* in H37Rv and the complemented strain (Δ*sigD attB*::*sigD*) was nearly identical, as determined by quantitative RT-PCR using RNAs isolated from broth cultures at two different time points (OD_{600} = 0.4 and 0.6) (not shown).

To identify genes regulated by SigD in *M. tuberculosis*, we performed a whole-genome transcription analysis by using microarrays to compare the transcription profiles of the Δ*sigD* mutant and the parental strain H37Rv. A comparison of transcription in these two strains, using a conservative error model with an FDR of <0.05, revealed a total of 471 genes that differed between the wt and the *sigD* mutant. Of these, 265 showed significantly decreased expression in the *sigD* mutant and 206 showed increased expression in the mutant. This number of affected genes represents about 10% of the total *M. tuberculosis* genome. Table 1 shows the 47 genes whose expression was ≥1.7 times higher in the wt than in the *sigD* mutant. Among these, hypothetical genes of unknown function were the most common. *sigD* and its adjacent 3′ gene (Rv3413c), Rv1815, Rv1816, *rpfC* and its adjacent 3′ gene (Rv1883c), and *iniB* and its 3′ genes showed the highest expression ratios. Also notable among the genes showing high expression ratios were several major chaperone/heat shock genes. Among the genes whose expression was significantly increased in the Δ*sigD* strain relative to H37Rv, PE-PGRS (proline glutamate [PE] motif and polymorphic GC-rich sequence) family genes, hypothetical genes of unknown function, and genes involved in cell wall processes and lipid metabolism were the most common (Table 2). See Table S1 in the supplemental material for a list of the 471 significantly regulated genes.

To verify that these results were effects of the mutation in *sigD*, we performed a microarray experiment comparing global transcription in the complemented strain with expression in the *sigD* mutant. Although some variation was observed in the rank order of the expression ratios, all of the genes that were most highly expressed in H37Rv relative to the Δ*sigD* strain were also highly expressed in the complemented strain relative to the Δ*sigD* strain (not shown). Rv3413c was among the genes that were highly expressed in the complemented strain, confirming the absence of a polar effect of the *sigD* mutation on this gene, which is immediately 3′ of *sigD* and expressed as part of an operon with *sigD*.

Identification of SigD-regulated promoters. To identify promoters that were likely to be directly regulated by SigD, we focused on those with the highest expression ratios (H37Rv/Δ*sigD* ratios). Primer extension experiments were performed with more than 20 candidate SigD-regulated genes. Three classes of promoters were identified. One group, represented by *sigD*, *rpfC*, and Rv1815, showed strong transcript signals in experiments using RNAs from H37Rv but no signal, even with prolonged exposure, in experiments using RNAs from the *sigD* mutant (Fig. 1A). In vivo transcription from these promoters is thus completely dependent on SigD. For each of these genes, no other strong promoter was identified within approximately 300 bases 5′ of the annotated initiation codon. For both *rpfC* and *sigD*, the *sigD*-dependent promoter is within the predicted coding sequence of these genes, indicating that the translation of these transcripts is initiated at a site 3′ of the annotated start codon (6). There are potential start codons 51 bases downstream of the experimentally determined 5′ end of the *sigD* transcript and 36 bases downstream of the 5′ end of the *rpfC* transcript. As for *M. tuberculosis*, an analysis of the *M. smegmatis sigD* locus identified a promoter that was active in the wt but absent from a *sigD* mutant strain (not shown).

A second class of SigD-regulated promoters was represented by *iniB* and *groEL2* (Fig. 1B). In these two cases, transcripts were identified that were present in experiments using wt RNAs and showed substantially decreased signals in experiments using RNAs from the Δ*sigD* strain. Thus, for these genes, expression from these promoters is partly regulated by SigD. In the case of *iniB*, a second transcript was present from a promoter whose activity did not differ between the wt and the *sigD* mutant, while for *groEL2* no other transcript was seen. It is not known whether this class of SigD-regulated promoters is directly recognized by SigD and also by a second sigma factor or whether the regulation by SigD is indirect. For the third set of genes examined by primer extension, we did not identify any transcripts that were consistently different between H37Rv and the *sigD* mutant (not shown).

By examining the regions 5′ of the beginning of the SigD-regulated transcripts, we sought to identify consensus promoter elements that might be recognized by SigD. A clear consensus −35 element was identified that was present in all of the promoters whose expression was completely SigD dependent (Fig. 2). A second region, separated by 16 bases from the 3′ end of the consensus, did not show a specific consensus sequence but had a higher than expected A+T content. Alignment of the partially SigD-regulated promoter of *iniB* showed

TABLE 1. Functional categories of genes with 1.7-fold more expression in *M. tuberculosis* H37Rv than in the *sigD* mutant strain

Gene family and name	Fold change	FDR	Product, its function, and additional comments
Regulatory			
Rv3414c	4.4	<0.001	SigD, ECF sigma factor
Rv3413c	2.8	<0.001	RsdA, probable anti-sigma factor
MT1932	8.0	<0.001	RpfC, resuscitation promoting factor
MT1931.1	2.6	<0.001	Downstream gene of *rpfC*, probable part of *rpfC* operon
Rv1883c	2.7	<0.001	Same as MT1931.1, except for a five-amino-acid gap
Rv1815	3.0	<0.001	Probable transcriptional regulation associated with Rv1816
Rv1816	1.7	0.008	Transcriptional regulatory protein, similar to *tetR* family
Heat shock response			
Rv0350	2.6	<0.001	DnaK, heat shock protein Hsp70
Rv0351	2.5	0.001	GrpE, Hsp70 cofactor, plays a role in adaptation
MT0366	2.3	0.008	Same as Rv0351
Rv0440	4.7	<0.001	GroEL2, chaperonin 2, prevents misfolding and promotes refolding
Rv3417c	2.1	<0.001	GroEL1, chaperonin 1, prevents misfolding and promotes refolding
Rv3418c	3.7	<0.001	GroES, chaperonin
Lipid metabolism			
MT0137	2.0	0.013	FbpC, fibronectin binding protein, required for biogenesis of cord factor, maintains cell wall integrity
MT0870	1.7	<0.001	LpqS, probable lipoprotein
MT1041	1.9	0.001	Putative polyketide synthase
Rv1182	1.7	<0.001	PapA3, probable polyketide synthase-associated protein
Rv1270	2.0	0.005	LprA, lipoprotein
Rv1750	1.9	<0.001	FadD1, fatty acid-CoA synthase
Rv2187	1.9	<0.001	FadD15, fatty acid CoA synthase, involved in fatty acid degradation
Cell wall process			
Rv0341	7.2	0.001	IniB, INH-inducible protein
Rv0342	2.4	<0.001	IniA, INH-inducible protein
Rv1860	1.8	0.001	ModD, fibronectin attachment protein
Rv2301	1.8	0.004	Probable cutinase, hydrolysis cutin
Rv3890c	1.8	0.002	EsxC, ESAT-6-like protein 11
Rv3891c	2.4	0.004	EsxD, ESAT-6-like protein
Intermediary metabolism and respiration			
MT0455	1.8	<0.001	Probable dehydrogenase
Rv2455c	1.7	0.048	Possible oxidoreductase
Rv3914	2.2	0.035	TrxC, thioredoxin, participates in various redox reactions
Adaptation			
Rv3846	2.5	0.002	SodA, superoxide dismutase A, involved in detoxification and adaptation
Unknown function			
MT0196	1.9	<0.001	Hypothetical protein
MT1020	1.8	<0.001	Hypothetical protein
MT1628	1.9	0.025	Hypothetical protein
MT2422	1.8	0.004	PPE family proteins
MT2890	1.9	<0.001	CRISPR-associated protein, TM1811 family
MT3258	2.2	<0.001	Hypothetical protein
Rv0257c	2.0	0.041	Hypothetical protein
Rv0276	2.0	<0.001	Hypothetical protein
Rv0309	1.7	0.004	Conserved exported protein
Rv1687c	1.9	<0.001	Hypothetical protein
Rv1779c	1.7	0.050	Hypothetical integral membrane protein
Rv2159c	1.7	0.007	Hypothetical protein
Rv2348c	1.7	0.008	Hypothetical protein
Rv2633c	2.1	<0.001	Hypothetical protein
Rv2699c	1.9	0.001	Hypothetical protein
Rv2822c	1.9	<0.001	Hypothetical protein
Rv3169	1.7	<0.001	Hypothetical protein
Rv3354	2.3	<0.001	Hypothetical protein
Rv3614c	2.0	0.001	Hypothetical protein
Rv3615c	2.2	<0.001	Hypothetical protein
Rv3675	1.8	0.002	Membrane protein

TABLE 2. Functional categories of genes with 1.7-fold more expression in the *M. tuberculosis sigD* mutant strain than in strain H37Rv

Gene family and name	Fold change	FDR	Product, its function, and additional comments
Adaptation			
Rv3811	1.7	0.001	Cold shock protein
Rv3648	1.8	0.004	Cold shock protein A
Rv3268	1.9	<0.001	Seems to be coregulated with CSPA-related protein Rv3267 (ratio = 1.5, FDR = 0.002)
Rv3269	1.9	<0.001	Heat shock protein, chaperonin, seems to be coregulated with Rv3267 and RV3268
Lipid metabolism			
Rv1094	2.4	<0.001	DesA2, Acyl-[ACP]-desaturase
Rv3229	4.4	<0.001	DesA3, linolenoil CoA desaturase
Cell wall process			
MT1416	2.0	0.001	Desaturase-related protein
Rv1614	2.2	<0.001	Lgt, prolipoprotein diacylglyceryl transferase
Rv1312	1.7	0.001	Secreted protein
Rv3920c	2.3	<0.001	Jag-like protein, involved in cell division
Regulatory			
Rv0823c	2.5	<0.001	Transcriptional regulatory protein
Rv1297	2.2	<0.001	Rho, transcription termination factor, Rho homologue
Rv0704	1.8	0.002	RplB, 50S ribosomal protein, peptidyltransferase activity
Respiration			
Rv3230c	1.9	<0.001	Oxidoreductase
Rv1644	2.1	<0.001	TsnR, 23S rRNA methyltransferase
Unknown			
Rv0516c	1.8	0.036	Hypothetical protein
Rv2393	1.8	0.001	Hypothetical protein
Rv3212	2.1	<0.001	Hypothetical protein
Rv3376	1.9	<0.001	Hypothetical protein
Rv3647c	1.7	0.001	Hypothetical protein
PE-PGRS family			
Rv0124	2.4	0.004	PE-PGRS 2
MT0132	2.3	0.02	PE-PGRS 2
Rv0834c	2.2	0.001	PE-PGRS 14
MT1123	2.1	0.001	PE-PGRS 22
Rv1396c	2.1	0.008	PE-PGRS 25
Rv1450c	1.9	<0.001	PE-PGRS 27
MT1499	1.8	0.002	PE-PGRS 28
Rv2490c	2.0	0.001	PE-PGRS 43
Rv3344c	2.1	<0.001	PE-PGRS 49
Rv3345c	2.2	<0.001	PE-PGRS 50
MT3612	1.9	<0.001	PE-PGRS 53
MT3615.3	2.7	0.021	PE-PGRS 57
MT3615.1	2.3	0.023	PE-PGRS
MT3448	2.1	0.001	PE-PGRS
MT3582	1.7	<0.001	PPE 19

moderate similarity to the consensus −35 sequence of the other SigD-dependent promoters. We did not identify any clear similarity to this consensus in the *groEL2* promoter region. This strong consensus identified in the promoters that were completely SigD dependent suggests that these promoters are directly recognized by the RNA polymerase holoenzyme incorporating SigD ($E\sigma^D$).

To attempt to identify additional promoters that might be directly regulated by SigD, we performed pattern searching with the −35 consensus sequence by using the search algorithm on the TubercuList web server (http://genolist.pasteur.fr/TubercuList). Although several partial matches were identified, none of the genes 3′ of these sequences were present among the genes whose expression was significantly decreased in the *sigD* mutant relative to H37Rv. Similarly, motif searching with the Bioprospector program (http://bioprospector.stanford.edu) of the 200 bases upstream and downstream of the start codons of the other genes with significantly decreased expression in the *sigD* mutant did not reveal additional sequences that matched the −35 consensus. Taken together, these data suggest that SigD directly regulates a relatively small number of genes and that much of the effect on transcription seen in the microarray experiments is likely to be indirect.

Growth and viability of Δ*sigD* strain and expression of *sigD* during growth and oxygen depletion. Our observation that *rpfC* is regulated by SigD led us to examine the growth and viability

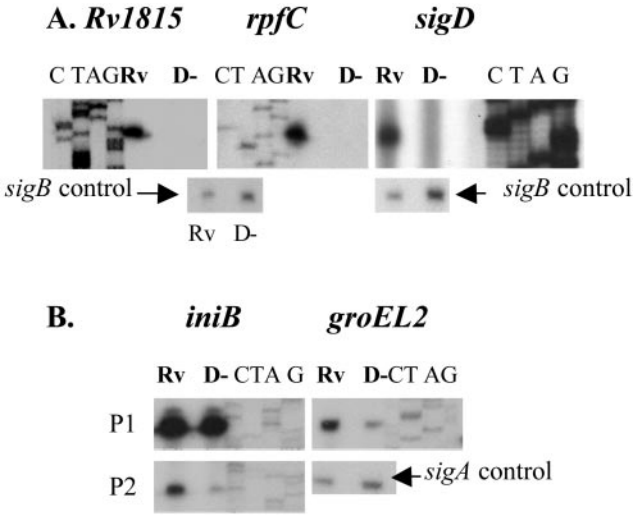

FIG. 1. Primer extension analysis was performed with genes whose expression was increased in H37Rv relative to the Δ*sigD* strain to identify in vivo transcription start sites. RNAs were isolated from exponential-phase cultures of H37Rv (Rv) or the Δ*sigD* strain (D−) of *M. tuberculosis*. Sequencing ladders shown adjacent to each transcript were generated with the same primers as those used for RT. The results for promoters that were completely (A) or partially (B) SigD dependent are shown. Control experiments demonstrating *sigA* or *sigB* transcripts were performed with each RNA tested.

of *M. tuberculosis* in broth culture and in response to oxygen depletion. On several occasions, when we inoculated cultures from frozen stocks or from colonies, the *sigD* mutant strains of *M. smegmatis* or *M. tuberculosis* appeared to take longer to become visibly turbid, suggesting an effect of SigD on viability or the lag phase. We were unable, however, to document a consistent difference in lag phase between the mutant and the wt in growth experiments in liquid medium, and no difference in exponential growth was observed (Fig. 3A). A comparison of the viabilities of long-term frozen cultures, measured by plating on solid medium, also showed no differences between H37Rv and the *sigD* mutant strain. During the course of gradual uniform oxygen depletion in the Wayne model of sealed stirred cultures, the *sigD* mutant strain showed a decrease in viability that was similar to those of H3Rv and the complemented strain (Fig. 3B). A strain that overexpressed *sigD* from a replicating plasmid in H37Rv also showed exponential growth and hypoxic survival that were not significantly different from those of the parental H37Rv and *sigD* mutant strains (not shown).

Two research groups have previously shown that *sigD* expression increases in response to starvation (3, 8). To further examine the possible role of SigD on growth and viability, we measured the expression of *sigD* during exponential growth and stationary phase and in response to oxygen depletion. As shown in Fig. 4A, *sigD* was expressed at a relatively high level throughout exponential growth and during stationary phase. This pattern closely followed the pattern of expression of *sigA*, the gene encoding the primary sigma factor of *M. tuberculosis*. These results are consistent with dot blot hybridization experiments showing the stable expression of *sigD* in exponential- and stationary-phase cultures (12). In cultures that were gradually depleted of oxygen, *sigD* expression decreased rapidly and to a greater extent than did *sigA* expression (Fig. 4B). The onset of this shift coincided with an increase in the expression of *hspX*, indicating that this change in expression occurred at a time when sufficient oxygen depletion had occurred to initiate the hypoxic response in these cultures.

Expression of resuscitation promoting factor genes in H37Rv and the Δ*sigD* strain. We identified *rpfC* as one of the genes that is likely to be directly regulated by SigD. *M. tuberculosis* has five *rpf* genes, and a recent study showed that the inactivation of *rpfC*, or any of the other individual *rpf* genes, did not have a measurable effect on growth, suggesting a possible redundancy of function of these genes (21, 30). We therefore measured the relative expression of all of the *M. tuberculosis rpf* genes in the wt and the *sigD* mutant strain, using quantitative real-time PCR, to see if there was a compensatory effect on the expression of any of the other *rpf* genes. As shown in Fig. 5, *rpfC* was by far the most abundant resuscitation promoting factor gene in *M. tuberculosis*; its mRNA level was approximately 50- to 500-fold higher than those of the other *rpf* genes. In this assay, the wt expressed about 100 times more *rpfC* than the Δ*sigD* mutant, consistent with the results from microarray experiments. Although no significant difference in the expression of *rpfB* or *rpfD* was seen between the Δ*sigD* mutant and H37Rv, small (four- to fivefold) but reproducible increases in the levels of *rpfA* and *rpfE* mRNAs were observed in the Δ*sigD* mutant.

Response to oxidative stresses and INH. Several alternative sigma factors of *M. tuberculosis* have been shown to play a role in the mycobacterial stress response, through alterations in survival following stress and through changes in gene expression in response to stress (9, 10, 13, 17–19, 24, 34). Although our microarray data did not suggest an obvious link to stress, we examined the role of *sigD* under a limited number of stresses by using a previously described disk diffusion assay. No consistent differences were observed between H37Rv and the Δ*sigD* mutant in experiments testing susceptibilities to the su-

```
                                  -35                  -10
Mt sigD     CGGTGGATGCTGGCGTACCGCTTAAAACGCGGTTGGGCCGTTATGGTCGATCCGGGAGTT
Ms sigD     AGTGTCGGTGCCAAGTAACGCTGGAGAGATCGCCCACGATGACAAGTTCGGGAGACCGTC
rpfC        ACTCTCTCTAATCGGTAACGCTTCGGCCACTTCCGGCGATATGTCGAGCATGACAGAATC
Rv1815      CTGGTCACGTCTCGGTAACGTCGCGACCCGACATTGCGAAAGTATTACCGTCGGGTTTTG
Consensus   ----------GTAACGct----------------------------------------
iniB        GTGAGGCGGAATCCATAGCGTCGATGGCACAGCGCCGGTCACGCCGGCGAACAGCTTCTT
```

FIG. 2. Alignment of promoter regions from the completely SigD-dependent in vivo promoters shown in Fig. 1 plus the experimentally defined SigD-dependent promoter of *M. smegmatis* (Ms-*sigD*). A strong consensus sequence in the −35 region is evident (bold letters), and an AT-rich −10 element is also present (underlined). Below the consensus line, the *iniB* P2 promoter, which is partially SigD dependent, is shown.

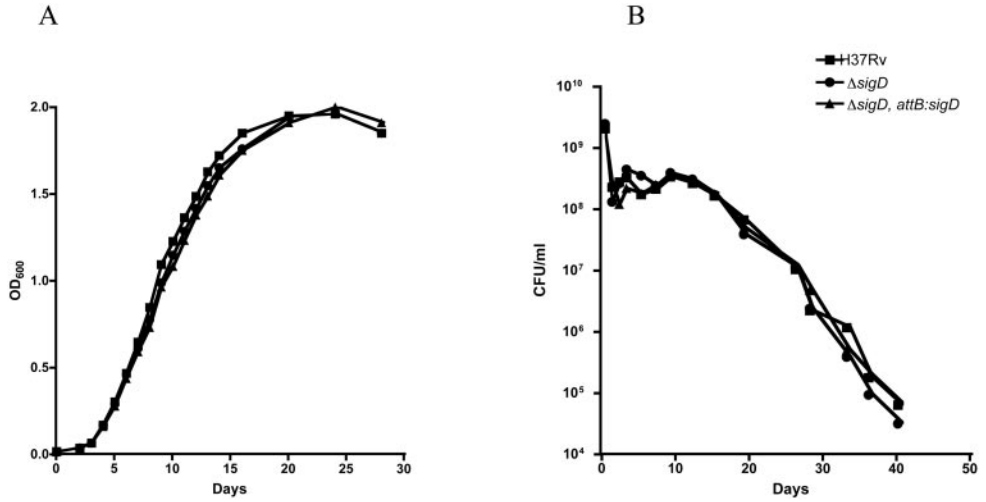

FIG. 3. (A) Growth kinetics of *M. tuberculosis* H37Rv, the Δ*sigD* mutant, and the Δ*sigD* complemented strain, as determined in Middlebrook 7H9 broth supplemented with ADC and 0.05% Tween 80 incubated at 37°C. OD_{600} values were measured at serial time points for 4 weeks. (B) Survival of *M. tuberculosis* H37Rv, the Δ*sigD* mutant, and the Δ*sigD* complemented strain in an oxygen depletion system. Seventeen-milliliter samples of early-log-phase cultures (OD_{600} = 0.3) were placed in 25-ml sealed bottles to obtain a headspace ratio of 0.5. Aliquots were removed for CFU determinations and were plated in duplicate on Middlebrook 7H11 medium at serial time points for 40 days.

peroxide-generating agent plumbagin, the organic peroxide cumene hydroperoxide, or the disulfide stress agent diamide. Based on our observation that SigD regulates the *iniBAC* operon, we examined the susceptibility of these strains to INH by using disk diffusion experiments and by examining their plating efficiencies on medium containing 0.05 μg of INH/ml. Although the disk diffusion assays did not show a consistent difference, a small (two- to fourfold) but reproducible decrease in the plating efficiency of the *sigD* mutant was observed in the presence of INH (not shown).

To examine the effect of INH on *iniB* expression and the role of SigD in the transcription of this gene, we performed primer extensions with RNAs from H37Rv and the Δ*sigD* mutant, with and without INH induction (Fig. 6). By phosphorimager analysis of the primer extension products (confirmed by quantitative RT-PCR), we observed a twofold induction of *sigD* expression following exposure to 1 μg of INH/ml. For *iniB*, in agreement with previous results (1), we observed a significant induction of transcription from the previously identified *iniB* promoter (P1 in our experiments) in response to INH (1). In addition, however, we observed substantial basal transcription from this promoter. A strong INH-induced induction of this transcript was observed in both H37Rv and the Δ*sigD* strain. Transcription from the partially SigD-dependent promoter that we identified (P2) was also strongly induced in response to INH, and this induction was blunted in the Δ*sigD* mutant.

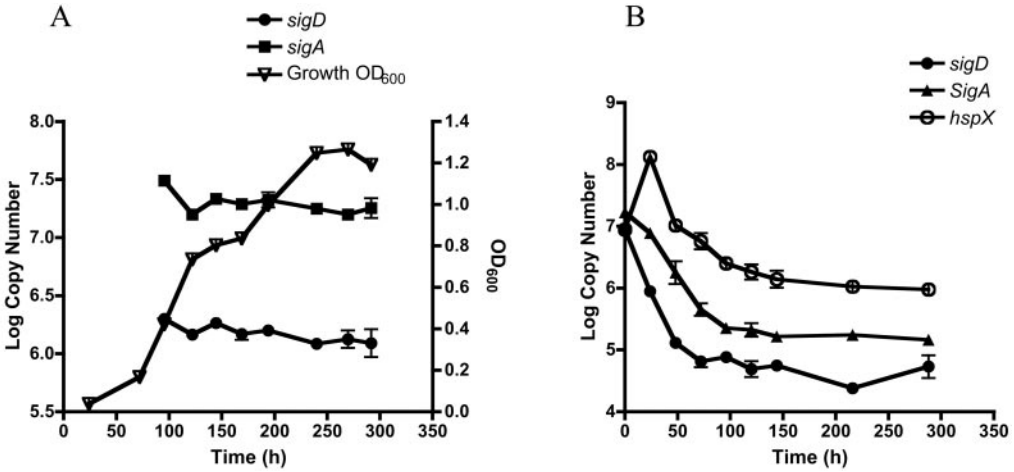

FIG. 4. Expression of *sigD* mRNA in *M. tuberculosis* H37Rv, as measured by quantitative real-time RT-PCR during exponential growth and stationary phase (A) and during gradual oxygen depletion (B). Aliquots were removed at each time point, RNAs were isolated, and RT-PCRs were performed with 100 ng of RNA as described in Materials and Methods. Quantification of *sigA* mRNA was performed with an aliquot of the same RNA preparation at each time point. For the oxygen depletion experiments, *hspX* mRNA was quantified as a control for hypoxia. For each gene, the relative copy number was determined by use of a standard curve of H37Rv genomic DNA. Errors bars indicate standard errors of the means.

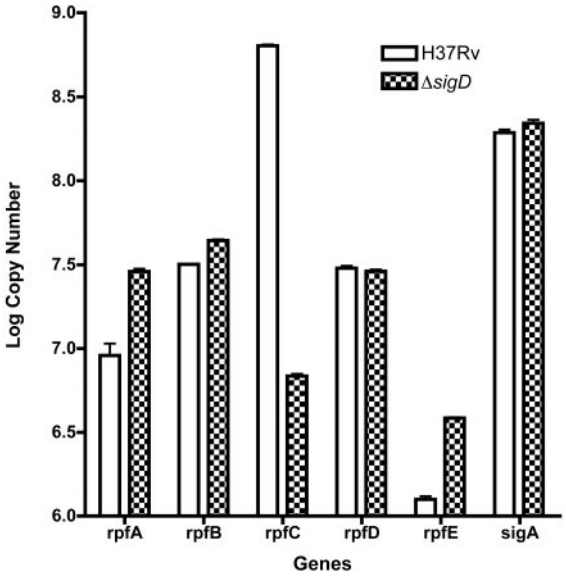

FIG. 5. Expression of each of the five *M. tuberculosis rpf* gene mRNAs during exponential growth, as measured in H37Rv and the Δ*sigD* strain by quantitative real-time RT-PCR. RNAs were isolated, and RT-PCRs were performed with 100 ng of RNA as described in Materials and Methods. Quantification of *sigA* mRNA was performed on aliquots of the same RNA preparations. Errors bars indicate standard errors of the means.

These data indicate that INH induction of the *iniB* operon occurs from two promoters, one of which is partially SigD dependent, suggesting that distinct mechanisms of induction may affect the activities of these two promoters.

Virulence analysis of *M. tuberculosis sigD* mutant. To assess the role of SigD in *M. tuberculosis* virulence, we used a mouse model of infection. BALB/c mice infected intravenously with the Δ*sigD* mutant displayed significantly prolonged survival relative to those infected with the parental H37Rv strain ($P < 0.001$ for the mutant versus the wt) (Fig. 7). Median survival times of 119, 164, and 149 days were obtained for the groups of mice infected with H37Rv, the Δ*sigD* mutant, and the complemented strain, respectively. In a second experiment, the median survival times of mice infected with H37Rv and the Δ*sigD* mutant were 117 and 151 days, respectively ($P < 0.005$).

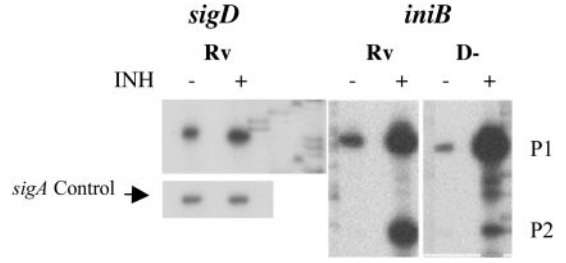

FIG. 6. Primer extension analysis of *sigD* and *iniB* promoters in response to INH exposure. Cultures of H37Rv (Rv) and Δ*sigD* (D−) were grown to mid-log phase and split into two aliquots, and INH was added to one aliquot to a final concentration of 1 μg/ml. The cells were harvested after 4 hours for RNA isolation, and primer extension experiments were performed with primers specific for *sigD*, *iniB*, or *sigA* (control).

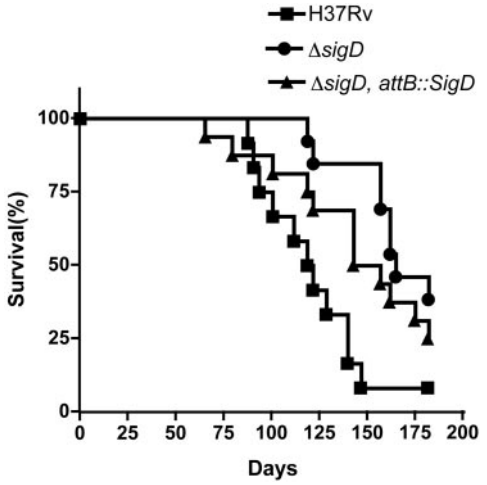

FIG. 7. Survival of mice infected with *M. tuberculosis* H37Rv, the Δ*sigD* mutant, and the Δ*sigD* complemented strain. BALB/c mice were infected by lateral tail vein injections with 10^6 CFU. Morbidity and weights were monitored throughout the experiment, and mice that became moribund were sacrificed. Twelve mice were infected in each group.

We examined the ability of these three *M. tuberculosis* strains to proliferate and persist in the tissues of BALB/c mice after intravenous infection with 10^6 CFU. The organ bacterial burdens in lungs and spleens were assessed by plating dilutions of the organ homogenates on days 1, 9, 24, and 59 after infection (Fig. 8). Although the inoculum sizes of the three strains varied less than twofold, as determined by plating on the day of infection, the bacterial burdens in the lungs measured on day 1 postinfection varied substantially, whereas very similar numbers of organisms were present in the spleens. The initial growth kinetics of the three strains were similar, although H37Rv appeared to replicate at a slightly higher rate between days 9 and 24, resulting in higher numbers of bacteria in both lungs and spleens on day 24. This difference persisted at 8 weeks in the lungs, with a slight decrease in the CFU in spleens of the Δ*sigD* and complemented strains during this plateau phase.

Hematoxylin and eosin-stained lung tissues from infected BALB/c mice were compared for their extents of tissue pathology. On day 24, the wt- and Δ*sigD* mutant-infected lung tissues showed similar degrees of lung pathology characterized by lymphocytic infiltration and a diffuse inflammation of the alveoli (Fig. 9A and E). On day 59, whole-lung cross sections showed extensive consolidation of the lung tissues from wt-infected mice (Fig. 9B). In the Δ*sigD* mutant-infected lungs, less diseased tissue and individual granulomatous lesions could be appreciated, and there appeared to be some resolution of the inflammatory response compared to day 24 (Fig. 9F). At a higher magnification, the wt-infected lung tissue showed extensive consolidation and lymphocytic infiltration, with almost no healthy lung tissue (Fig. 9C). In contrast, the Δ*sigD* mutant-infected lung tissue had significant areas of healthy lung space interspersed with smaller rounded granulomatous lesions (Fig. 9G). The wt-infected tissue had numerous monocytoid cellular infiltrates, consistent with the presence of macrophages, in addition to extensive lymphocyte infiltration (Fig. 9D). The

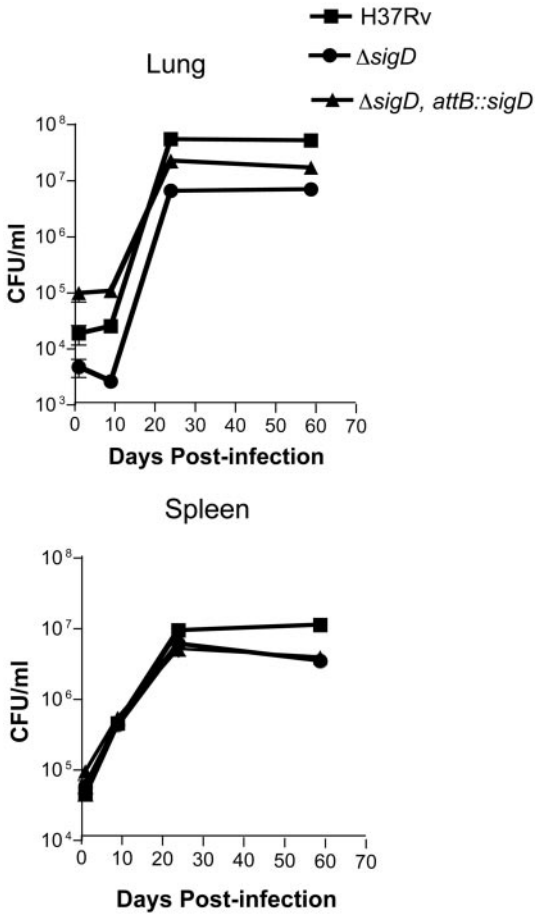

FIG. 8. Replication and persistence of *M. tuberculosis* H37Rv, the Δ*sigD* mutant, and the Δ*sigD* complemented strain in mice. BALB/c mice were infected by lateral tail vein injections with 10^6 CFU, mice were sacrificed on days 1, 9, 24, and 59, and plating for bacterial burdens in the lungs and spleens was performed as described in Materials and Methods.

Δ*sigD* mutant-infected lesions had a less intense lymphocyte infiltration and exhibited inflamed alveolar tissue with maintenance of some of the structural integrity of the alveoli (Fig. 9H).

DISCUSSION

In this paper, we have shown that the *M. tuberculosis* alternative sigma factor SigD regulates a large number of genes, based on global transcription analysis, but that it appears to regulate relatively few genes directly. The breadth of the effect of SigD on transcription is likely mediated through its control of other regulators of transcription and through molecules that alter other cell processes, which then affect transcription indirectly. Among the SigD-controlled proteins, RpfC, Rv1816, and Rv3413c are likely to affect transcription. Though the function of Rv1816 has not been determined, sequence-based annotation indicates that it is a *tetR* family transcription factor. This gene is located immediately 3′ of Rv1815, a gene of unknown function whose promoter we have shown to be completely SigD dependent, and it appears to be part of an operon with Rv1815 based on similarities in their expression patterns. Similarly, Rv3413c is located immediately 3′ of *sigD* and is expressed as part of an operon from the SigD-dependent *sigD* promoter. Although it is also not functionally characterized, the protein encoded by this gene may function as a regulator of SigD activity, e.g., an anti-sigma factor. With predicted intra- and extracellular domains linked by a single transmembrane region, this protein may function to control SigD activity in response to extracellular or membrane-localized signals.

The resuscitation promoting factor RpfC may play a major role in the broad transcriptional effects observed in the *sigD* mutant. Our data and previous reports indicate that *rpfC* is the most highly expressed of the *rpf* genes (21, 30); here we have shown that its expression is highly dependent on SigD. Previous data indicated that RpfC is the second most potent of the *M. tuberculosis* Rpf proteins (21). Despite this observation, we were unable to identify strong effects of *sigD* inactivation on growth or survival under a variety of conditions. These results are similar to those of Tufariello et al., who were unable to identify growth phenotypes in any of the individual *rpf* mutant strains that they constructed (30). These data suggest a redundancy of function of the *M. tuberculosis* Rpf proteins. This interpretation is supported by our finding that *rpfA* and *rpfE* expression is increased in the *sigD* mutant strain, a result that suggests a compensatory mechanism regulating *rpf* expression in this strain. RpfA appears to be the most potent of the Rpf proteins, achieving a maximal reduction of lag phase in a *Micrococcus* resuscitation assay at concentrations that were 100-fold lower than those of RpfC, the second most potent *M. tuberculosis* Rpf in this assay (21). The relatively small increase in the expression of *rpfA*, together with this large difference in potency, could explain the lack of a consistent effect on lag phase of the *sigD* mutation in our experiments. Our data indicate that neither *rpfA* nor any of the *rpf* genes are other than *rpfC* is regulated by SigD.

Based on in vivo promoters that we identified among the genes that were most highly regulated by SigD, we identified a likely consensus recognition sequence for promoters transcribed by $E\sigma^D$. Like many other extracytoplasmic-function sigma factors (16), the main specificity for promoter recognition by SigD lies in the −35 region, where an eight-base consensus sequence was identified. In addition, an A+T-rich region is present at the optimal distance from the −35 element for a −10 promoter element and is therefore likely to contribute to the activities of these promoters. The SigD-regulated *iniB* promoter that we identified contains a region with some similarity to the SigD −35 consensus, but it lacks the −10 A+T-rich element. Whether this promoter is directly recognized by SigD in vivo is not certain. If it is, this would suggest that a broader range of promoters may be transcribed by $E\sigma^D$. Our inability to identify additional SigD-regulated in vivo promoters in more than 20 additional genes examined by primer extension, however, suggests that this is not the case. Interestingly, the SigD-regulated promoter of *iniB* is distinct from the *iniB* promoter identified by Alland et al. (1). In addition to confirming the induction by INH of the expression of this operon from the previously identified SigD-independent promoter, we determined that *iniB* expression from the partially SigD-dependent promoter is also induced by INH and that this induction is largely SigD dependent.

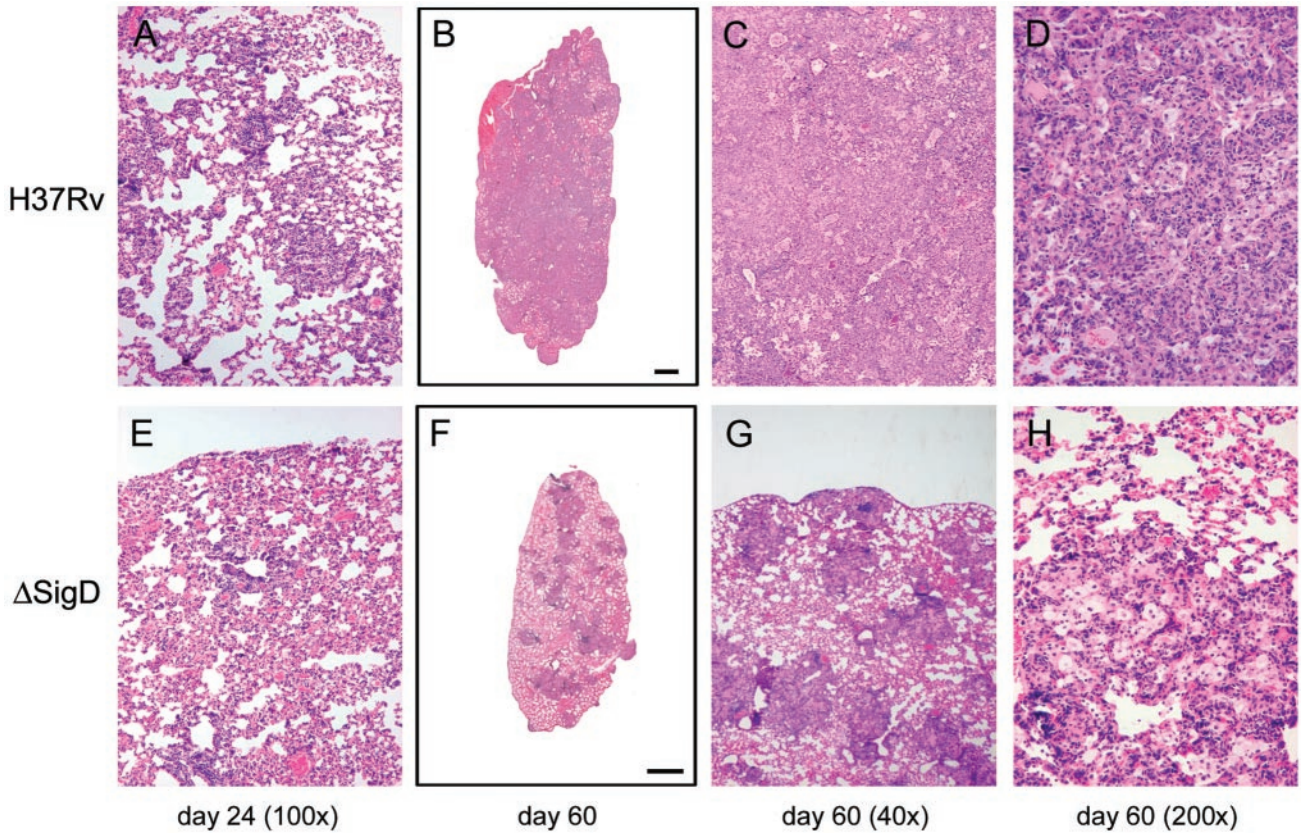

FIG. 9. Histopathology of lungs of BALB/c mice infected with *M. tuberculosis* H37Rv or the Δ*sigD* strain. The images show hematoxylin and eosin staining of lung sections from mice infected with H37Rv (A to D) or the Δ*sigD* mutant (E to H). The time points at which the mice were sacrificed are indicated below the columns of panels.

Our analysis of *sigD* expression showed that there is a moderately high level of expression throughout the exponential phase and into stationary phase, a result that is consistent with the dot blot data of Hu and Coates (12). Under hypoxic conditions resulting from gradual oxygen depletion, we found that the expression of *sigD* declined rapidly and to a larger degree than the expression of *sigA*, coincident with the onset of the hypoxic response, as indicated by the increased expression of *hspX*. In contrast, the expression of *sigD* was not found to be strongly affected in previously reported microarray experiments investigating gene expression after a rapid shift to hypoxic conditions (27). The expression of *sigD* was, however, significantly decreased following infection of both quiescent and activated macrophages (26).

The expression of *sigD* has been found to be significantly regulated, based on microarray analyses, in two other settings. Betts et al. found that *sigD* expression was increased two- to threefold 24 and 96 h after a shift to starvation conditions (3). Dahl et al. identified *sigD* and *rpfC* as having significantly increased expression in the wt relative to a *relA* mutant of *M. tuberculosis* in log-phase cultures, and they also showed that *sigD* and *rpfC* were up-regulated in response to starvation (8). Our data showing that the promoters of *sigD* and *rpfC* are SigD dependent indicate that the Rel-dependent starvation-induced expression of these genes is likely mediated via SigD. Consistent with this interpretation, the starvation-induced expression of *sigD* was blunted in a *relA* mutant strain, suggesting that *sigD* is part of the *relA* regulon. These results do not exclude an additional independent regulation of *sigD* expression under other conditions. These data, together with the stable, relatively high-level expression of *sigD* during growth and early stationary phase in our studies and those of Hu and Coates, suggest roles for SigD both in nutrient-replete growth conditions and in the adaptation to starvation or stringent response physiology, an apparent paradox that remains to be further defined.

In addition to *sigD*, Rv3413c, *rpfC*, Rv1815, and Rv1816, other genes that were up-regulated in the wt relative to the *sigD* mutant included several chaperone genes and genes involved in lipid metabolism and cell wall processes. SigD regulates gene expression for optimal growth in the absence of oxygen limitation, which might occur early during infection in vivo. Other sigma factors, most notably SigH, have been shown to regulate chaperone gene expression in response to oxidative and heat stress (24). In the setting of rapid growth in the absence of stress, the induction of chaperone expression regulated by SigD may be more important for nascent protein folding than for disaggregation and degradation or refolding of proteins that have been damaged by stress.

The genes whose expression was increased in the *sigD* mutant may also provide insight into SigD function. Most striking was the large number of genes encoding PE-PGRS family

proteins. These genes represented >40% of the genes that were most highly expressed in the *sigD* mutant relative to H37Rv. It was interesting that several PE-PGRS family genes were also up-regulated in a *relA* mutant (8). The function of this large family of genes remains unknown, but some of them have been shown to be expressed in granulomas and to play a role in mycobacterial virulence (23). It has been hypothesized that this family of proteins may be important for immune modulation or surface interactions, and evidence indicates that members of this family of proteins are expressed at the cell surface and recognized by the immune system (2, 4, 28). The fact that the expression of many of these genes is repressed by SigD indicates that they are expressed in settings in which *sigD* expression is decreased. One such setting is during infection of both quiescent and activated macrophages (26), raising the possibility that these PE-PGRS genes may be important for bacterial survival during the early stages of infection.

We observed a moderate but significant decrease in the virulence of the *sigD* inactivated strain, with associated small decreases in replication in vivo. The most notable differences in histopathology occurred after the onset of immunity, as 8-week specimens showed more extensive inflammation in the lungs of mice infected with the wt than in those infected with the mutant. Differences in survival, replication, and histopathology are likely linked to the decreased expression of *sigD* in the mutant, although the partial complementation of survival and the lack of clear complementation of in vivo replication make this conclusion less certain. Whether the specific expression of one or a few key SigD-dependent genes causes this phenotype or whether it is the result of a more global disruption of growth regulation is not known. The less severe virulence phenotype of the *sigD* mutant relative to the *relA* mutant (8) indicates that SigD-dependent gene expression may account for part, but not all, of the virulence defect of the *relA* mutant.

The stable expression of *sigD* during exponential growth and stationary phase, the RelA-dependent increased expression of *sigD* in response to starvation, the down-regulation of *sigD* during macrophage infection and hypoxia, and the regulation by SigD of *rpfC*, which is thought to play a role in the renewal of growth after starvation or stationary phase, suggest a complex interaction of signals mediated by SigD and other regulators that allows *M. tuberculosis* to adapt its growth physiology during infection. The opposite effects on *sigD* expression of starvation versus hypoxia are particularly striking. These data suggest that these conditions are encountered at distinct stages or sites during infection and that activation or repression of the *sigD* regulons is important for *M. tuberculosis* adaptation in these settings. Since *M. tuberculosis* encounters a broad range of environmental conditions during infection, fine-tuning of its physiology by a large number of regulatory signals, including those mediated by SigD and other alternative sigma factors, is undoubtedly required to allow growth and survival in vivo. Further insight into the interplay of these regulatory networks should ultimately lead to a more integrated understanding of the pathogenesis of tuberculosis.

ACKNOWLEDGMENTS

This work was supported by Public Health Service grant AI 37901 from the National Institute of Allergy and Infectious Diseases to R.N.H. and by a fellowship from the Warren Whitman Richardson fund to R.H. Oligonucleotide microarrays were provided by the Institute for Genomic Research through the NIAID-sponsored Pathogen Functional Genomics Resource.

We thank Xiaoling Puyang for excellent technical assistance, Eric Rubin for the generous gift of DNA microarrays, Eric Rubin, Chris Sassetti, and Seby L. Edassery for assistance with microarray methods and analysis, and Michael Brenner for the use of biosafety level 3 facilities.

REFERENCES

1. **Alland, D., A. J. Steyn, T. Weisbrod, K. Aldrich, and W. R. Jacobs, Jr.** 2000. Characterization of the *Mycobacterium tuberculosis iniBAC* promoter, a promoter that responds to cell wall biosynthesis inhibition. J. Bacteriol. **182:** 1802–1811.
2. **Banu, S., N. Honore, B. Saint-Joanis, D. Philpott, M. C. Prevost, and S. T. Cole.** 2002. Are the PE-PGRS proteins of *Mycobacterium tuberculosis* variable surface antigens? Mol. Microbiol. **44:**9–19.
3. **Betts, J. C., P. T. Lukey, L. C. Robb, R. A. McAdam, and K. Duncan.** 2002. Evaluation of a nutrient starvation model of *Mycobacterium tuberculosis* persistence by gene and protein expression profiling. Mol. Microbiol. **43:** 717–731.
4. **Brennan, M. J., G. Delogu, Y. Chen, S. Bardarov, J. Kriakov, M. Alavi, and W. R. Jacobs, Jr.** 2001. Evidence that mycobacterial PE_PGRS proteins are cell surface constituents that influence interactions with other cells. Infect. Immun. **69:**7326–7333.
5. **Chen, P., R. E. Ruiz, Q. Li, R. F. Silver, and W. R. Bishai.** 2000. Construction and characterization of a *Mycobacterium tuberculosis* mutant lacking the alternate sigma factor gene *sigF*. Infect. Immun. **68:**5575–5580.
6. **Cole, S. T., R. Brosch, J. Parkhill, T. Garnier, C. Churcher, D. Harris, S. V. Gordon, K. Eiglmeier, S. Gas, C. E. Barry III, F. Tekaia, K. Badcock, D. Basham, D. Brown, T. Chillingworth, R. Connor, R. Davies, K. Devlin, T. Feltwell, S. Gentles, N. Hamlin, S. Holroyd, T. Hornsby, K. Jagels, and B. G. Barrell.** 1998. Deciphering the biology of *Mycobacterium tuberculosis* from the complete genome sequence. Nature **393:**537–544.
7. **Curcic, R., S. Dhandayuthapani, and V. Deretic.** 1994. Gene expression in mycobacteria: transcriptional fusions based on *xylE* and analysis of the promoter region of the response regulator *mtrA* from *Mycobacterium tuberculosis*. Mol. Microbiol. **13:**1057–1064.
8. **Dahl, J. L., C. N. Kraus, H. I. Boshoff, B. Doan, K. Foley, D. Avarbock, G. Kaplan, V. Mizrahi, H. Rubin, and C. E. Barry III.** 2003. The role of RelMtb-mediated adaptation to stationary phase in long-term persistence of *Mycobacterium tuberculosis* in mice. Proc. Natl. Acad. Sci. USA **100:**10026–10031.
9. **DeMaio, J., Y. Zhang, C. Ko, D. Young, and W. Bishai.** 1996. A stationary-phase stress-response sigma factor from *Mycobacterium tuberculosis*. Proc. Natl. Acad. Sci. USA **93:**2790–2794.
10. **Fernandes, N., Q.-L. Wu, D. Kong, X. Puyang, S. Garg, and R. Husson.** 1999. A mycobacterial extracytoplasmic function sigma factor involved in survival following heat shock and oxidative stress. J. Bacteriol. **181:**4266–4274.
11. **Geiman, D. E., D. Kaushal, C. Ko, S. Tyagi, Y. C. Manabe, B. G. Schroeder, R. D. Fleischmann, N. E. Morrison, P. J. Converse, P. Chen, and W. R. Bishai.** 2004. Attenuation of late-stage disease in mice infected by the *Mycobacterium tuberculosis* mutant lacking the SigF alternate sigma factor and identification of SigF-dependent genes by microarray analysis. Infect. Immun. **72:**1733–1745.
12. **Hu, Y., and A. R. Coates.** 2001. Increased levels of *sigJ* mRNA in late stationary phase cultures of *Mycobacterium tuberculosis* detected by DNA array hybridisation. FEMS Microbiol. Lett. **202:**59–65.
13. **Kaushal, D., B. G. Schroeder, S. Tyagi, T. Yoshimatsu, C. Scott, C. Ko, L. Carpenter, J. Mehrotra, Y. C. Manabe, R. D. Fleischmann, and W. R. Bishai.** 2002. Reduced immunopathology and mortality despite tissue persistence in a *Mycobacterium tuberculosis* mutant lacking alternative sigma factor, SigH. Proc. Natl. Acad. Sci. USA **99:**8330–8335.
14. **Kerr, M. K., M. Martin, and G. A. Churchill.** 2000. Analysis of variance for gene expression microarray data. J. Comput. Biol. **7:**819–837.
15. **Lee, M., L. Pascopella, W. Jacobs, Jr., and G. Hatfull.** 1991. Site-specific integration of mycobacteriophage L5: integration-proficient vectors for *Mycobacterium smegmatis*, *Mycobacterium tuberculosis* and bacille Calmette-Guerin. Proc. Natl. Acad. Sci. USA **88:**3111–3115.
16. **Lonetto, M., K. Brown, K. Rudd, and M. Buttner.** 1994. Analysis of the *Streptomyces coelicolor sigE* gene reveals the existence of a subfamily of eubacterial RNA polymerase σ factors involved in the regulation of extracytoplasmic functions. Proc. Natl. Acad. Sci. USA **91:**7573–7577.
17. **Manganelli, R., E. Dubnau, S. Tyagi, F. R. Kramer, and I. Smith.** 1999. Differential expression of 10 sigma factor genes in *Mycobacterium tuberculosis*. Mol. Microbiol. **31:**715–724.
18. **Manganelli, R., M. I. Voskuil, G. K. Schoolnik, E. Dubnau, M. Gomez, and I. Smith.** 2002. Role of the extracytoplasmic-function sigma factor sigmaH in *Mycobacterium tuberculosis* global gene expression. Mol. Microbiol. **45:**365–374.

19. **Manganelli, R., M. I. Voskuil, G. K. Schoolnik, and I. Smith.** 2001. The *Mycobacterium tuberculosis* ECF sigma factor sigmaE: role in global gene expression and survival in macrophages. Mol. Microbiol. **41:**423–437.
20. **McKinney, J. D., K. Honer zu Bentrup, E. J. Munoz-Elias, A. Miczak, B. Chen, W. T. Chan, D. Swenson, J. C. Sacchettini, W. R. Jacobs, Jr., and D. G. Russell.** 2000. Persistence of *Mycobacterium tuberculosis* in macrophages and mice requires the glyoxylate shunt enzyme isocitrate lyase. Nature **406:**735–738.
21. **Mukamolova, G. V., O. A. Turapov, D. I. Young, A. S. Kaprelyants, D. B. Kell, and M. Young.** 2002. A family of autocrine growth factors in *Mycobacterium tuberculosis*. Mol. Microbiol. **46:**623–635.
22. **Pelicic, V., M. Jackson, J.-M. Reyrat, W. J. Jacobs, B. Gicquel, and C. Guilhot.** 1997. Efficient allelic exchange and transposon mutagenesis in *Mycobacterium tuberculosis*. Proc. Natl. Acad. Sci. USA **94:**10955–10960.
23. **Ramakrishnan, L., N. A. Federspiel, and S. Falkow.** 2000. Granuloma-specific expression of Mycobacterium virulence proteins from the glycine-rich PE-PGRS family. Science **288:**1436–1439.
24. **Raman, S., T. Song, X. Puyang, S. Bardarov, W. Jacobs, Jr., and R. Husson.** 2001. The alternative sigma factor SigH regulates major components of the oxidative and heat stress responses in *Mycobacterium tuberculosis*. J. Bacteriol. **183:**6119–6125.
25. **Sassetti, C. M., D. H. Boyd, and E. J. Rubin.** 2003. Genes required for mycobacterial growth defined by high density mutagenesis. Mol. Microbiol. **48:**77–84.
26. **Schnappinger, D., S. Ehrt, M. I. Voskuil, Y. Liu, J. A. Mangan, I. M. Monahan, G. Dolganov, B. Efron, P. D. Butcher, C. Nathan, and G. K. Schoolnik.** 2003. Transcriptional adaptation of *Mycobacterium tuberculosis* within macrophages: insights into the phagosomal environment. J. Exp. Med. **198:**693–704.
27. **Sherman, D. R., M. Voskuil, D. Schnappinger, R. Liao, M. I. Harrell, and G. K. Schoolnik.** 2001. Regulation of the *Mycobacterium tuberculosis* hypoxic response gene encoding alpha-crystallin. Proc. Natl. Acad. Sci. USA **98:**7534–7539.
28. **Singh, K. K., X. Zhang, A. S. Patibandla, P. Chien, Jr., and S. Laal.** 2001. Antigens of *Mycobacterium tuberculosis* expressed during preclinical tuberculosis: serological immunodominance of proteins with repetitive amino acid sequences. Infect. Immun. **69:**4185–4191.
29. **Snapper, S., R. Melton, S. Mustafa, T. Kieser, and W. Jacobs, Jr.** 1990. Isolation and characterization of efficient plasmid transformation mutants of *Mycobacterium smegmatis*. Mol. Microbiol. **4:**1911–1919.
30. **Tufariello, J. M., W. R. Jacobs, Jr., and J. Chan.** 2004. Individual *Mycobacterium tuberculosis* resuscitation-promoting factor homologues are dispensable for growth in vitro and in vivo. Infect. Immun. **72:**515–526.
31. **Voskuil, M. I., D. Schnappinger, K. C. Visconti, M. I. Harrell, G. M. Dolganov, D. R. Sherman, and G. K. Schoolnik.** 2003. Inhibition of respiration by nitric oxide induces a *Mycobacterium tuberculosis* dormancy program. J. Exp. Med. **198:**705–713.
32. **Wayne, L. G., and L. G. Hayes.** 1996. An in vitro model for sequential study of shiftdown of *Mycobacterium tuberculosis* through two stages of nonreplicating persistence. Infect. Immun. **64:**2062–2069.
33. **World Health Organization.** 2002. Tuberculosis fact sheet. World Health Organization, Geneva, Switzerland.
34. **Wu, Q.-L., D. Kong, K. Lam, and R. Husson.** 1997. A mycobacterial extracytoplasmic function sigma factor involved in survival following stress. J. Bacteriol. **179:**2922–2929.